

Application News

MALDI-TOF Mass Spectrometry Analysis MALDI-7090

MALDI Imaging and Segmentation Analysis of Human Inflammatory Bowel Disease (IBD) using the MALDI-7090 and IMAGEREVEAL™ MS

Simona Salivo

User Benefits

- ◆ High speed and high spatial resolution imaging analysis on the MALDI-7090 enabled an accurate reproduction of the colon architectural structure at near-cellular level.
- ◆ Segmentation analysis using intuitive IMAGEREVEAL MS software identified significant areas corroborated by microscopy findings.

■ Introduction

Inflammatory bowel diseases (IBD) such as ulcerative colitis (UC) and Crohn's disease (CD) are chronic and relapsing inflammatory conditions of unknown aetiology. Current treatments are not universally effective and can have severe adverse effects. Therefore, early detection and precise identification of the type of disease is important in order to apply the correct treatment.

Colon tissue is complex and contains different types of cells, and therefore a cell-specific analytical tool is required to improve diagnosis and prognosis. MALDI imaging mass spectrometry of lipids may facilitate this, as the signature and distribution of molecules that may help identify the metabolic stage of the tissues, can be obtained directly from tissue sections.

While MALDI imaging analysis combined with optical microscopy can provide valuable insight into the molecular species that are responsible for the pathological alteration

of tissue structures, a more advanced data mining by means of computational methods may be required for a better, thorough understanding of the metabolic changes that characterise IBD diseases. Segmentation analysis is a popular computational method that is often used in conjunction with MALDI imaging data.

Here, we present an imaging mass spectrometry study of endoscopic biopsies obtained from patients with IBD acquired at 10 micron (µm) spatial resolution using the Shimadzu MALDI-7090 MALDI TOF-TOF mass spectrometer, combined with the Shimadzu IMAGEREVEAL MS imaging analysis software for data and segmentation analysis (Fig. 1). The high spatial resolution capability of the MALDI-7090 was key for resolving the main colon tissue structures (crypts, lamina propria and muscularis mucosae), while the segmentation analysis enabled identification of both areas of inflammation and the nuclei component of the colonocytes, based on the microscopy analysis.

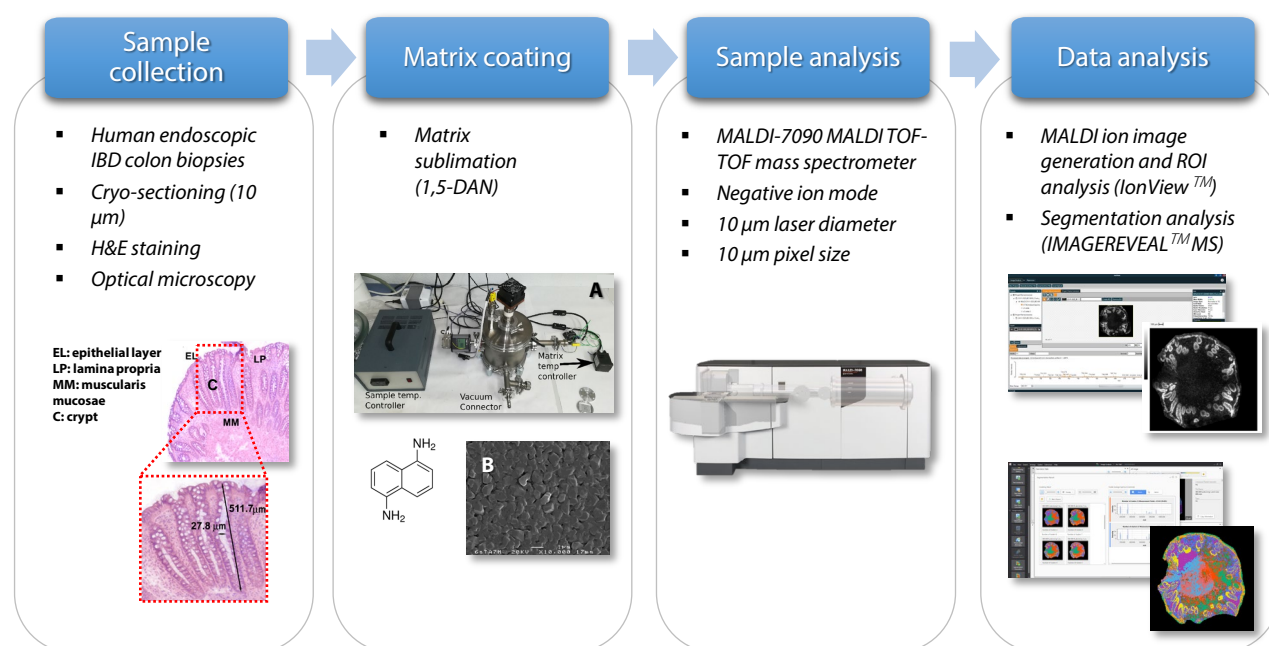


Fig. 1 Analytical workflow for the MALDI imaging and data analysis of human endoscopic IBD colon biopsies. H&E images taken from [1]. A: stainless-steel sublimator. B: SEM image of the 1,5-DAN crystals at x10,000 magnification, showing an average crystal size of ~3 µm [2].

■ Sample Preparation and Analysis Conditions

Samples of excised human colon tissue were kindly provided by the Institut d'Investigació Sanitària Illes Balears (IdISBa), Palma, Balearic Islands, Spain. The sample collection for the study was specifically approved by the Ethics Research Committee of the Balearic Islands (IB 2118/13 PI). Tissue samples were snap frozen in liquid nitrogen and cryo-sectioned at 10 μm thickness. Sections were covered with 1,5-diaminonaphthalene (DAN) for negative-ion detection using a stainless-steel sublimator and imaged using the Shimadzu MALDI-7090 MALDI TOF-TOF mass spectrometer (10 μm laser spot diameter, 10 μm pixel size). Data were processed using the IonView™ imaging software (Shimadzu) to obtain the MALDI ion images and perform region of interest (ROI) analysis. Segmentation analysis was carried out using IMAGEREVEAL MS imaging data analysis software (Shimadzu).

■ Results – MALDI imaging and ROI analysis (IonView)

The fast acquisition speed of the MALDI-7090 enabled the interrogation of whole sections in a reasonably short time (less than an hour, ~ 40,000 pixels) at 10 μm /pixel. Fig. 2A shows the negative mode MALDI imaging spectrum of a typical IBD sample, where the arachidonic acid-containing PI(38:4) (m/z 885) is, expectedly, one of the most abundant species. It is worth mentioning that, in addition to its role as a precursor in the biosynthesis of eicosanoids (a family of inflammation metabolites), arachidonic acid is closely involved with colonocyte differentiation as well as with its potential malignization (tumour formation). Fig. 2B shows the MALDI ion images of the m/z 861.550 (PI(36:2)) and 885.550 (PI(38:4)) species from healthy (top) and diseased (bottom) tissues of an ulcerative colitis patient, alongside the consecutive H&E stained sections. The lamina propria, epithelium (crypts) and muscularis mucosae tissues are clearly distinguishable. The lining of the crypts is composed of a single-cell monolayer, the structure of which is clearly visible in the ion images thanks to the 10 μm imaging capability of the MALDI-7090 and optimised sample preparation. The overlay of the m/z 861.550 and 885.550 ions (Fig. 2B) demonstrates how these species are specific to the crypts and lamina propria, respectively.

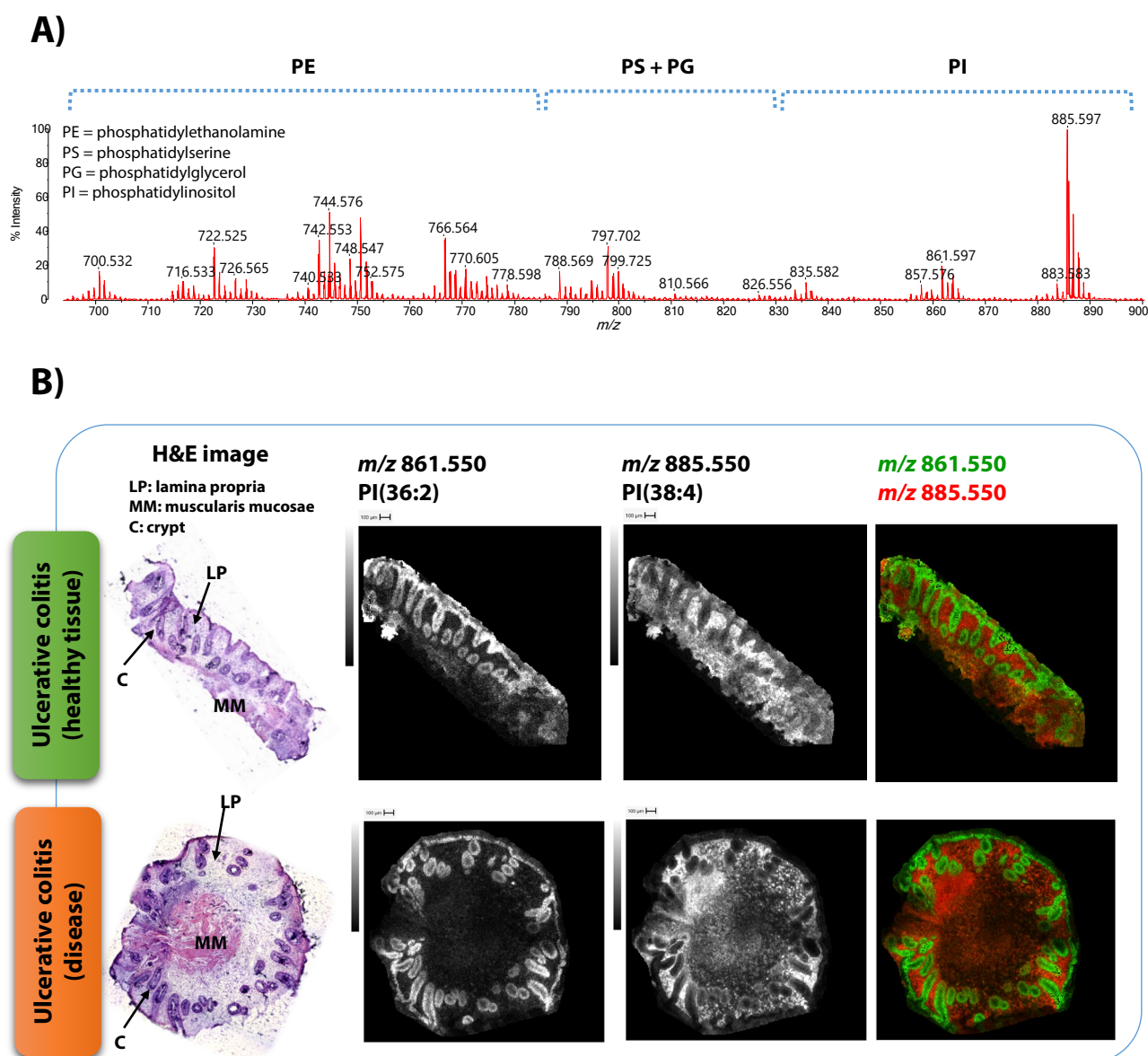


Fig. 2 A) Negative mode MALDI spectrum of a typical IBD sample: PE, PS, PG and PI phospholipid classes are mainly present. B) H&E and MALDI ion images of the m/z 861.550 and 885.550 species, which are specific to the crypts and lamina propria, respectively. The identity of the m/z 861.550 and 885.550 species were confirmed by MALDI-MS/MS analysis acquired on-tissue (data not shown).

Fig. 3 shows the ROI spectra of the crypts (top) and lamina propria (bottom) of the IBD diseased tissue, obtained with the IonView software. It can be observed how the two profiles appear different and are unique of the tissue type.

A more in-depth analysis of the epithelium tissue unveiled the presence of a gradient of intensities of some phosphatidylinositol (PI) species along the crypts. It has been described in [3] that the epithelial cell monolayer invaginates (i.e. folds in on itself) into the lamina propria to form the crypt. Adult stem cells reside at the base of the crypt and gradually differentiate to mature colonocytes as they ascend towards the lumen (Fig 4A). During this process, the lipidome changes to reflect the differentiation process.

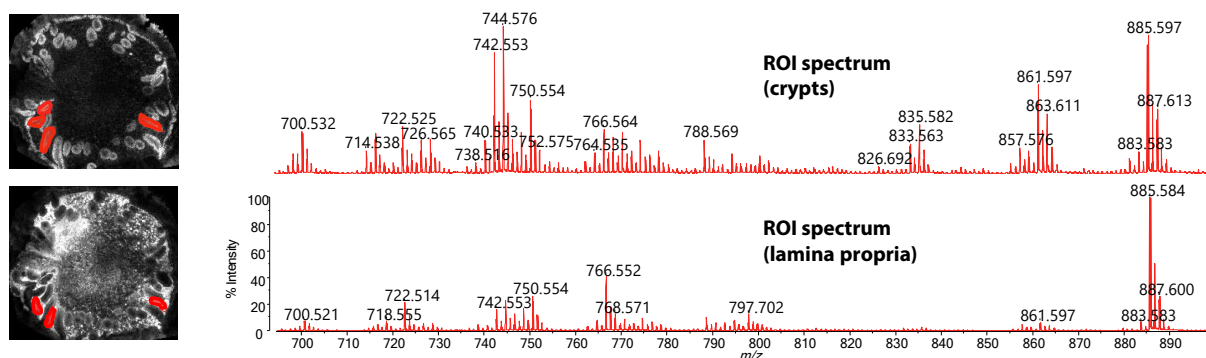


Fig. 3 Left: ROI regions corresponding to the crypts (top) and lamina propria (bottom). Right: ROI spectrum of crypts (top); ROI spectrum of lamina propria (bottom). ROI images and spectra obtained using IonView software.

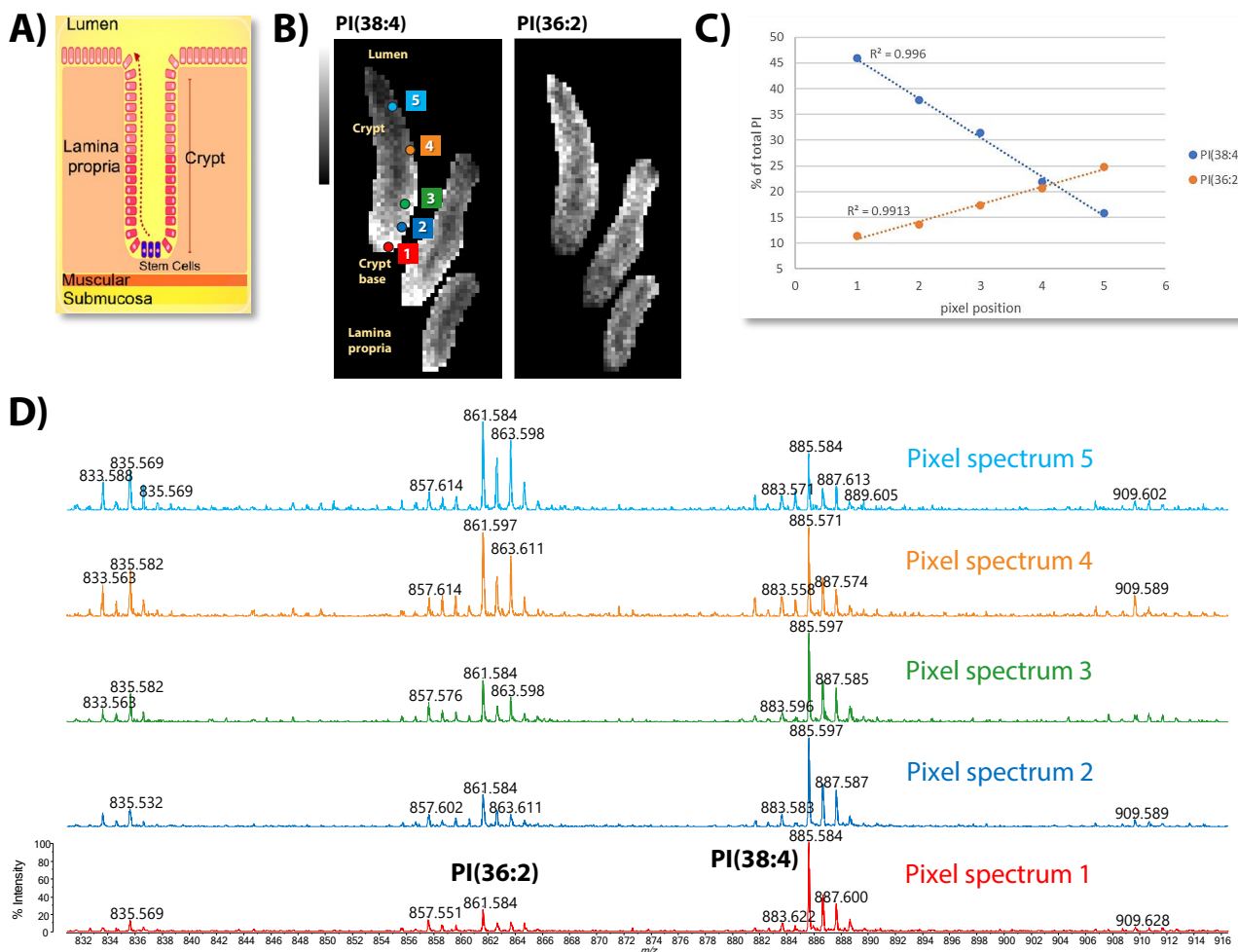


Fig. 4 A) Schematic representation of a colon crypt and the colonocytes differentiation process [2]. B) Distribution of PI(38:4) and PI(36:2) species along the crypt (ROIs corresponding to the crypts were drawn in the MALDI image to expose the gradients). Coloured dots: positions of the pixel spectra retrieved along the length of the crypt for calculation of intensity percentages. C) PI(38:4) and PI(36:2) levels, expressed as percentage (%) of the total PI per pixel position, showing the linearity of the variations. D) Pixel spectra retrieved along the crypt showing the PI class. The changes in the lipidome along the crypt are clearly observable going from the base to the lumen.

Fig. 4B shows the gradients of PI(38:4) and PI(36:2) species along the crypt, obtained through an ROI analysis of the crypts. Five pixel spectra were retrieved along the length of the crypt to assess the behaviour of the changes in expression of the PI class (Fig. 4D). Fig. 4C shows the plot of the PI(38:4) and PI(36:2) levels, expressed as percentage (%) of the total PI, per pixel position. This showed a decrease of the arachidonic acid-containing species [PI(38:4)] and an increase in the diunsaturated fatty acid-containing species [PI(36:2)], moving from the base of the crypt towards the lumen, in agreement with what was observed in [3]. The variation of these lipids fitted into a linear regression, with high correlation coefficients (R^2).

■ Results – Segmentation analysis (IMAGEREVEAL MS)

Segmentation analysis was carried out in IMAGEREVEAL MS software, using the City Block algorithm and after careful optimisation of the binning, denoising, number of clusters settings. Fig. 5A shows the result of the microscopy analysis carried out by a pathologist, highlighting the area of infiltration by lymphocytes, a class of immune cells. This abnormal infiltration is a clear symptom of chronic tissue inflammation. The segmentation image, obtained with 11 clusters, enabled not only the main tissue structures (crypts, lamina propria and muscularis mucosae) to be grouped, but also to identify the area corresponding to the infiltrates (Fig. 5B).

Furthermore, the segmentation analysis unveiled the presence of an epithelial cluster that anatomically correlates with the nuclear component of the colonocyte monolayer (yellow cluster; Fig. 5C). It is worth noting that the size of the nucleus is 9-12 μm , hence the high spatial resolution of 10 μm achieved played a significant role in the successful separation of the nuclear cluster from the rest of the crypt, thus reaching a near-cellular resolution [4].

■ Conclusion

In this study, we demonstrated how the changes in lipid expression that characterise IBD disease can be identified thanks to the powerful combination of: 1) an optimised

sample preparation; 2) MALDI imaging analyses at high speed and high spatial resolution (10 μm) with the MALDI-7090 mass spectrometer; 3) imaging data and segmentation analysis using the IonView and IMAGEREVEAL MS imaging software. The high quality imaging data generated by the MALDI-7090 allowed the architectural structure of the colon to be accurately reproduced. The segmentation analysis proved to be a powerful aid in support of the microscopy analysis in confirming the area containing a high density of immune infiltrates, with the additional benefit of obtaining the molecular signature.

■ References

- [1] Anal. Bioanal. Chem. (2015) 407: 4697–4708.
- [2] Anal. Chem. (2019) 91: 803–807.
- [3] Biochim Biophys Acta (2016) 1861: 1942–1950.
- [4] Anal. Bioanal. Chem. (2019) 411(30): 7935–7941.

■ Acknowledgements

We would like to thank Dr. Gwendolyn Barceló-Coblijn (Institut d'Investigació Sanitària Illes Balears (IdISBa), Palma) and Prof. Jose A. Fernandez (University of the Basque Country (UPV/EHU), Spain) for preparing and providing the imaging samples used in this study and for their contributions with the analysis of the imaging data.

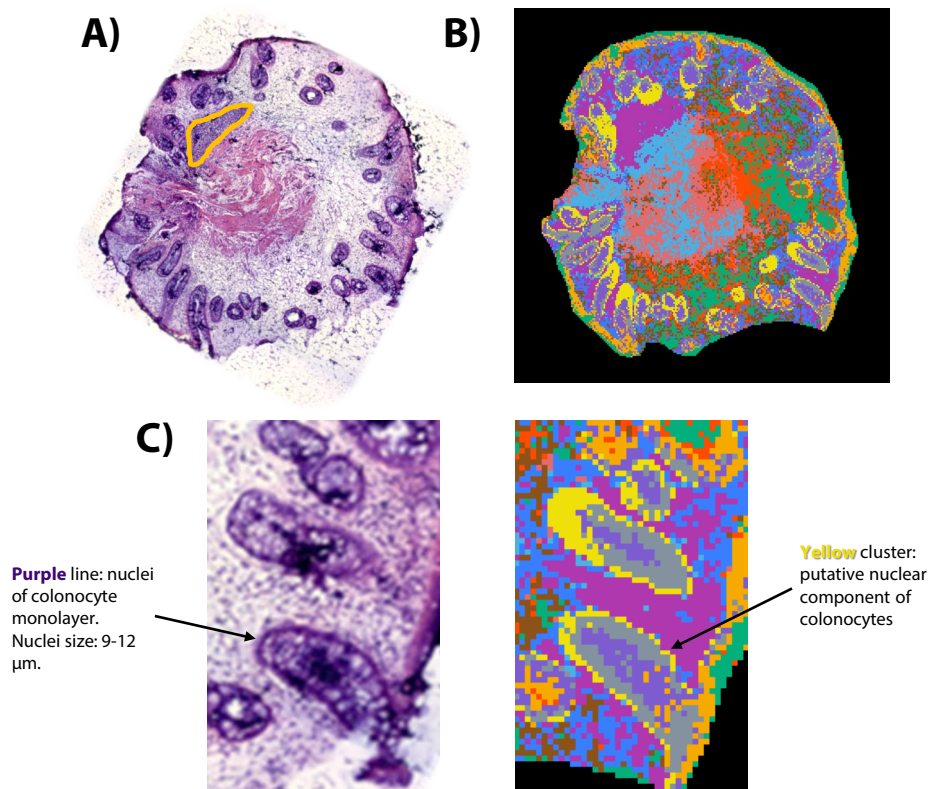


Fig. 5 A) H&E image of the IBD diseased tissue highlighting the area of infiltration by lymphocytes, as determined by a pathologist. B) Segmentation image obtained with City Block algorithm and 11 clusters (IMAGEREVEAL MS): the main tissue structures (crypts, lamina propria and muscularis mucosae) as well as the area corresponding to the infiltrates are clearly distinguishable. C) Left: extract of the H&E image highlighting the nuclei of the single-cell epithelial monolayer, identified by the purple line (nuclei size: 9-12 μm). Right: extract of the segmentation image. The yellow cluster may correlate with the nuclear component of the colonocytes.

IMAGEREVEAL and IonView are trademarks of Shimadzu Corporation or its affiliated companies in Japan and/or other countries.



SHIMADZU

Shimadzu Corporation

www.shimadzu.com/an/

For Research Use Only. Not for use in diagnostic procedures.

This publication may contain references to products that are not available in your country. Please contact us to check the availability of these products in your country.

The content of this publication shall not be reproduced, altered or sold for any commercial purpose without the written approval of Shimadzu. See <http://www.shimadzu.com/about/trademarks/index.html> for details.

Third party trademarks and trade names may be used in this publication to refer to either the entities or their products/services, whether or not they are used with trademark symbol "TM" or "®".

Shimadzu disclaims any proprietary interest in trademarks and trade names other than its own.

The information contained herein is provided to you "as is" without warranty of any kind including without limitation warranties as to its accuracy or completeness. Shimadzu does not assume any responsibility or liability for any damage, whether direct or indirect, relating to the use of this publication. This publication is based upon the information available to Shimadzu on or before the date of publication, and subject to change without notice.

12-MO-487-EN

First Edition: Jan. 2023

Related Products

Some products may be updated to newer models.



> MALDI-7090
Matrix-Assisted Laser
Desorption/Ionization Time-o...

Related Solutions

> Tissue

> Price Inquiry

> Product Inquiry

> Technical Service /
Support Inquiry

> Other Inquiry